DOI: https://doi.org/10.14256/JCE.1225.2015
Građevinar 3/2017

Primljen / Received: 27.1.2015.
Ispravljen / Corrected: 8.5.2016.
Prihvaćen / Accepted: 21.11.2016.
Dostupno online / Available online: 10.4.2017.

Structural model calibration of RC structure with two-leaf cavity brick infill wall by deterministic approach

Authors:

Assist.Prof. Onur Onat, PhD. CE
Munzur University
Faculty of Civil Engineering
Tunceli, Turkey
onuronat@munzur.edu.tr

Prof. Paulo B. Lourenço, PhD. CE
ISISE, University of Minho
Faculty of Civil Engineering
Guimaraes, Portugal
pbl@civil.uminho.pt

Assoc.Prof. Ali Koçak, PhD. CE
Yıldız Technical University
Faculty of Civil Engineering
İstanbul, Turkey
akocak@yildiz.edu.tr

Original scientific paper

Onur Onat, Paulo B. Lourenço, Ali Koçak

Structural model calibration of RC structure with two-leaf cavity brick infill wall by deterministic approach

An adaptive solution for updating structural model of a RC structure with two-leaf cavity brick infill wall under flexible boundary problem is presented in this paper. The structure was simulated with Diana 9.4.4 finite element software. Next, an elastic foundation with interface elements was used to overcome this stiffness problem of the foundation. The validation of the structure was made with the optimization based modal updating using MATLAB. Five calibration types were performed and compared with experimental data.

Key words:
finite element method, reinforced concrete, two-leaf cavity brick infill wall, structural model updating

Izvorni znanstveni rad

Onur Onat, Paulo B. Lourenço, Ali Koçak

Deterministički pristup za kalibriranje modela ab konstrukcije s dvoslojnim šupljim zidom od opeke

U radu je prikazano prilagodljivo rješenje za kalibraciju modela AB konstrukcije s dvoslojnim šupljim zidom od opeke u svrhu rješavanja problema popustljivih rubnih uvjeta. Simulacija konstrukcije provedena je pomoću programa Diana 9.4.4 koji se temelji na metodi konačnih elemenata. Kako bi se uklonio problem krutosti u temeljima, usvojeni su elastični temelji s kontaktnim elementima. Provjera konstrukcije obavljena je modalnim kalibriranjem baziranim na optimalizaciji pomoću programa MATLAB. Analizirano je pet kalibracijskih tipova, a dobiveni su rezultati te uspoređeni s eksperimentalnim podacima.

Ključne riječi:
metoda konačnih elemenata, armirani beton, dvoslojni šuplji ispunski zid od opeke, kalibriranje modela

Wissenschaftlicher Originalbeitrag

Onur Onat, Paulo B. Lourenço, Ali Koçak

Deterministisch basierte Kalibration von Modellen für Stahlbetonkonstruktionen mit zweischaligen Mauerwerkswänden

In dieser Arbeit wird ein anpassungsfähiger Ansatz der Kalibration von Modellen für Stahlbetonkonstruktionen mit zweischaligen Mauerwerkswänden zur Berücksichtigung nachgiebiger Randbedingungen dargestellt. Die Konstruktion wurde mit dem Programm Diana 9.4.4 basierend auf der Finite-Elemente-Methode simuliert. Um das Problem steifer Fundationen zu umgehen, wurden mit Kontaktelementen elastische Auflager abgebildet. Die Prüfung der Konstruktion erfolgte aufgrund modaler Kalibration mit Optimierung im Programm MATLAB. Es wurden fünf Typen der Kalibration analysiert und Resultaten experimenteller Versuche gegenübergestellt.

Schlüsselwörter:
Finite-Elemente-Methode, Stahlbeton, zweischalige Mauerwerksausfachung, Kalibration von Modelen

1. Introduction

At the present time, the use of Finite Element (FE) methods for structural analysis problems has been validated and is commonly accepted by professional community. But reliability of a model, modelled with a finite element software, mostly depends on input parameters. Improving correlation between the FE simulation and experimental model using available measured data is known as model calibration or updating [1]. The aim of model calibration is to improve certainty of engineering properties of the FE model and to bring modelling assumptions of a specific FE model as close as possible to reality [2]. In other words, the main purpose of model calibration is to bypass unforeseen aspects related to modelling [3]. Various model errors can be found when comparing numerical results with experimental results:

- structural errors of the model (model structure errors), when a numerical model has some physical definition deficiencies and material model behaviour is weakly represented;
- model parameter errors, mostly related to incorrect simplification of model assumptions;
- model order errors, related to approximation of complex system during mesh creation [4-6].

Ramos et al. [7] used modal updating to overcome the model structural error. It was emphasized that this model error occurred due to partial soil settlement and it was overcome by using different interface elements under the structure. Li et al. [8] studied modal updating with incomplete modal data. A cross validation method was used to eliminate incomplete modal data, and the authors concluded that the modal updating process was implemented successfully, with less than 1 % of error. Sevim et al. [2] used modal calibration to eliminate the model parameter error in a historical masonry arch bridge to obtain correct structural analysis results. It was reported that an average natural frequency error was decreased from 15 % to 5 % with modal calibration [2]. Moreover, it was underlined in the same paper that higher maximum and minimum principal stress values were obtained before modal calibration [2]. Atamtürktür [9] investigated the model structure error due to simplification of complex geometry, and the model order error due to discretization of system during creation of mesh. The model structure error amounted to no more than 2 % due to properly simplified complex geometry, while the model order error ranged between 0.15 % and 0.5 % when the coarse mesh and fine mesh were used.

There are two types of calibration: one is the Deterministic Model Calibration and the other is the Stochastic Model Calibration. The deterministic calibration is a traditional method and it is the most widely used iteration type aimed at matching numeric results with experimental ones. The stochastic calibration is an iteration type that is used to obtain the closest possible response with uncertain physical measurements [9]. In this study, researchers were faced with the flexible boundary condition problem during the structural model calibration procedure. The flexible boundary condition problem means obtaining modal shapes with different sequence. This problem occurred due to degradation of stiffness at the level of foundations. The problem was observed during calculation of mode frequencies and mode shapes by a finite-element software. The first three mode shapes and frequencies were completely incorrect. This is not a common problem for huge structures and for shake table experiments. According to prior assessments of this problem, the specimen tested using the shake table is generally produced outside of the shake table. Then this constructed structure is transported to the shake table by crane to perform the dynamic identification test. The purpose of dynamic identification is to capture first five or more modal shapes and first five or more mode frequencies to calibrate the structural finite element model with correct parameters. The deterministic modal calibration was selected based on available experimental modal frequencies and shapes. This study presents an adaptive solution for flexible boundary condition by using elastic foundation and, after having used the elastic foundation, the first two mode shapes and mode frequencies were obtained in correct sequence. A total of four mode frequencies were updated. After updating, an average 5 % error was reduced to 2 %.

2. Theory and use of structural model updating

2.1. Model updating parameters

The accuracy and compatibility of modal calibration indicators are the most important issue during the updating process. Experimental and numerical results should be compared with each mode pair (frequency and mode shape) to fit the numeric model. This comparison should be performed with parameters such as the Modal Assurance Criterion (MAC), Coordinate Modal Assurance Criterion (COMAC) and Normalized Modal Differences (NMD) [4, 5]. The calculation of these parameters was conducted using natural frequencies and mode shapes (i.e. vectors). In this study, model updating indicators are directly calculated by these parameters and compared with available data. The advantages and disadvantages of different indicators are compared in Table 1.

2.1.1. Modal assurance criterion (MAC)

MAC is the cosine of the angle between numerical and experimental eigenvectors [10]. This criterion was developed on the basis of orthogonality to check if mode shapes are consistent. If the frequency response function matrix does not have enough information on the base of modal vector, the prediction of modal vector under different

Table 1. Advantage, disadvantage and selection reason of modal calibration indicators

Indicator	Advantage	Disadvantage	Reason for selection
MAC	Gives match ratio for each mode	Gives single indicator for estimated mode	Evaluation of mode shape match
COMAC	Gives match ratio for each measurement point	Contributes with a negative value with low MAC	Evaluation between correlation of FE and Experimental results at each node
NMD	Gives sensitive values for each node	Gives extremely high values, even if acceptable MAC values are observed	Evaluation of sensitivity for table measuring points

conditions become important to evaluate experimental data [11]. The purpose of using MAC in this study is to measure the linearity of numeric and experimental mode shapes as seen in eq. (1).

$$MAC_{e,n} = \frac{\left|\{\varphi_i^e\}^T \{\varphi_i^n\}\right|^2}{\{\varphi_i^e\}^T \{\varphi_i^e\}\{\varphi_i^n\}^T \{\varphi_i^n\}} \quad (1)$$

In eq. (1), $\{\varphi_i^e\}^T$ and $\{\varphi_i^n\}$ are mode vectors of two different models. One of them is experimental and the other one is numeric. The range of MAC value varies from 0 to 1. Zero means no match between the mode shapes, while one means that good correlation between the experimental and numeric modes has been established. Although in this parameter evaluation MAC is sensitive to high magnitudes, higher magnitudes have a dominant effect on erroneous points. So, erroneous points will have a minor effect. But these points have to be distributed well to the structure [11].

2.1.2. Coordinate modal assurance criterion (COMAC)

The coordinate modal assurance criterion is the extended version of the modal assurance criterion. MAC is a single value for a considered structure in terms of each mode, but there is more than one COMAC value for each selected degree of freedom, both in transverse and longitudinal direction, to compare experimental and numerical displacements and rotations. In this study, COMAC calculation was conducted by four selected nodes. These nodes were compared with the experimental model and numeric model. They were selected according to the data obtained experimentally on the structure. COMAC value is used in this study so as to obtain some detailed information, such as displacement and rotation of numeric model, under flexible boundary condition. These compared displacements and rotations show the consistency of the model with the experimental model. COMAC value can be calculated using eq. (2) as shown below [11].

$$COMAC_{i,e,n} = \frac{\sum_i^n \left|\varphi_{i,j}^e \varphi_{i,j}^n\right|^2}{\sum_i^n (\varphi_{i,j}^e)^2 \sum_i^n (\varphi_{i,j}^n)^2} \quad (2)$$

2.1.3. Normalized modal differences (NMD)

Normalized Modal Differences is a kind of parameter that depends on MAC value and is calculated by MAC value to check the discrepancy of two mode shape vectors. The difference from MAC is in sensitivity as presented in eq. (3). During a modal updating process, if a MAC value is lower than 0.9, NMD value will be higher. The reason for this situation lies in higher differences. The 0.99 MAC value corresponds to the 0.10 NMD value. This comparison shows the sensitivity of NMD. Less than 0.33 NMD value is evaluated a good correlation, considering the range of NMD values [12]:

$$NMD_{e,n} = \frac{\sqrt{1 - MAC_{e,n}}}{MAC_{e,n}} \quad (3)$$

2.2. Model updating techniques

2.2.1. Douglas&Reid method

This type of modal updating method is based on the minimization of differences between experimental and numerical modal frequencies. Selecting variables and constructing the finite element model before modal updating is not enough. Considering improper condition, upper and lower limit of estimations, are also important during the process. Douglas and Reid proposed the equation below [13]:

$$f_j^{FE}(X_1, X_2, \ldots\ldots, X_3) = C_i + \sum_{k=1}^{n} [A_{ik} X_k + B_{ik} (X_k)^2] \quad (4)$$

Where X_k (k=1,2,....., n) are variables to calibrate and A_{ik}, B_{ik} and C_i are constants. The (2n+1) constant must be calculated.

$$\begin{aligned} f_j^{FE}\left(X_1^B, X_2^B, \ldots\ldots, X_n^B\right) &= C_j + \sum_{k=1}^{n} [A_{ik} X_k^B + B_{ik} (X_k^B)^2] \\ f_j^{FE}\left(X_1^L, X_2^B, \ldots\ldots, X_n^B\right) &= C_j + \sum_{k=1}^{n} [A_{ik} X_k^L + B_{ik} (X_k^B)^2] \\ f_j^{FE}\left(X_1^U, X_2^B, \ldots\ldots, X_n^B\right) &= C_j + \sum_{k=1}^{n} [A_{ik} X_k^U + B_{ik} (X_k^B)^2] \end{aligned} \quad (5)$$

$$f\left(X_1^B, X_2^B, \ldots\ldots, X_n^L\right) = C_j + \sum_{k=1}^{n}[A_{ik}X_k^L + B_{ik}(X_k^L)^2]$$
$$f_j^{FE}\left(X_1^B, X_2^B, \ldots\ldots, X_n^U\right) = C_j + \sum_{k=1}^{n}[A_{ik}X_k^U + B_{ik}(X_k^U)^2] \quad (5)$$

In eq. (5), X_n^B refers to the base value (starting point), X_n^L refers to the lower boundary limit and X_n^U refers to the upper boundary limit. For instance, if there are two parameters for calibration, three constants should be calculated using an optimization software. After calculation of constants, the least square minimization is implemented on numeric frequencies f_j^{FE} and the experimental f_j^{EX}.

$$\pi = \sum_{i=1}^{m} w_i e_i^2 \quad (6)$$

$$\varepsilon_i = \sum_{i=1}^{m} f_i^{ex} - f_i^{FE}\ (X_1, X_2, \ldots, X_n) \quad (7)$$

where π is the objective function, ε_i is the residual function, w_i is the weight constant and m is the number of frequencies mentioned for modal updating [13].

2.2.2. Robust method

The basic idea behind calling this method Robust is to accomplish the objective function directly. This robust method is used by Ramos, 2007 [12] and is also applied in this study. The method is directly used by objective function π and the errors between numeric and experimental free vibration modes are demonstrated by f_{iE} and f_{iFE}. The differences between numeric and experimental displacements are shown by $\phi_{j,Exp}$ and $\phi_{j,FE}$. Moreover, the errors between numeric and experimental modal curvatures are demonstrated by $\phi''_{j,FE}$ and $\phi''_{j,Exp}$. Equation 8 is constructed using the following variables [12]:

$$\pi = \frac{1}{2}[W_w \sum_{i=1}^{m}(\frac{f_{i,FE}^{\ 2} - f_{i,Exp}^{\ 2}}{f_{i,Exp}^{\ 2}})^2 + W_{\varnothing}\sum_{i=1}^{m}(\varnothing_{i,FE} - \varnothing_{i,Exp})^2 + W_{\varnothing''}\sum_{i=1}^{n}(\frac{\varnothing''_{i,FE} - \varnothing''_{i,Exp}}{\varnothing''_{i,Exp}})^2 \quad (8)$$

In eq. (8), W_w, W_ϕ *and* $W_{\phi''}$ are the weight constants of natural frequencies, mode shapes, and modal curvatures, respectively. The weighing matrices have different values according to the engineering judgement of the analyser but, in order to account for the measurement and identification errors, they can be calculated with the inverse of the normal variance of each modal quantity [12]. Furthermore, m and j are the number of modes and modal displacement, respectively [12]. This updating process is conducted on the basis of optimization techniques. This optimization must be implemented by means of the Jacobian sensitivity matrix composed of i row and j column where the Gradient $\nabla\pi(\theta)$ is constructed. Then the Jacobian matrix is calculated by the first order partial derivative of residual functions. The Jacobian matrix is presented in eq. (9).

$$J(\theta)_{ji} = \frac{\partial\pi(\theta)}{\partial x_i} \quad (9)$$

After calculating the Jacobian matrix, the Hessian Matrix G is calculated from the second partial order derivatives of the residual function [8].

$$G(\theta)_{jk} = \frac{\partial^2\varepsilon_i(\theta)}{\partial x_i \partial x_j} \quad (10)$$

Where ε is the residual function and θ are updated variables. The Hessian and Gradient are the objective functions. These functions can be seen in the following form [12]:

$$\nabla\pi(\theta) = J(\theta)^T \cdot \pi(\theta) \quad (11)$$

$$\nabla^2\pi(\theta) = J(\theta)^T\, J(\theta) + Q(\theta \quad (12)$$

where

$$Q(\theta) = \sum_{i=1}^{m}\pi_i(\theta)G_i(\theta) \quad (13)$$

3. Two-Leaf cavity brick infill wall

3.1. Geometry and materials

The tested and therefore simulated structure is composed of two bays and two storeys. The dimensions of the structure are 3.80 x 4.30 x 4.0 m, and the structure is scaled to 1:1.5. The Two Leaf Cavity Wall (TLCW) used in the envelope is composed of the 9 cm outer wall leaf, 2 cm gap, and 7 cm inner wall leaf. Dimensions of the structure and infill wall are presented in Figure 1.

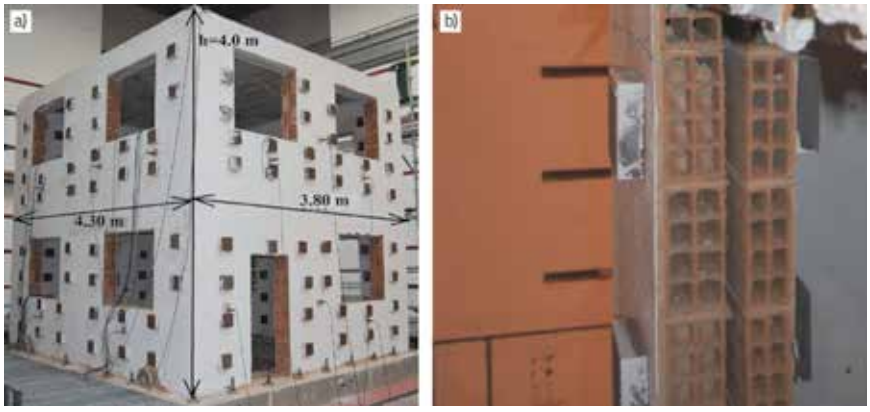

Figure 1. Simulated structure and infill wall components, a) dimensions of simulated structure, b) two leaf cavity infill wall [14]

Table 2. Engineering properties of concrete and Infill according to Two-Leaf Cavity Brick Wall Model

E_{conc} [MPa]	ν_{con}	ρ_{conc} [kg/m³]		E_{inf} [MPa]	ν_{inf}	ρ_{inf} [t/m³]	f_{cm} [MPa]	
		Number	ρ_1				Number	f_{cm}
		1	2190				1	26.5
30444	0.2	2	2200	3602.7	0.213	1.59	2	28.4
		3	2220				3	33.7
		Average	2203				Average	29.5

The total area is 15.18 m². The longitudinal and transverse directions measure 4.16 m and 3.65 m, respectively. The plan view of the tested model is shown in Figure 2.

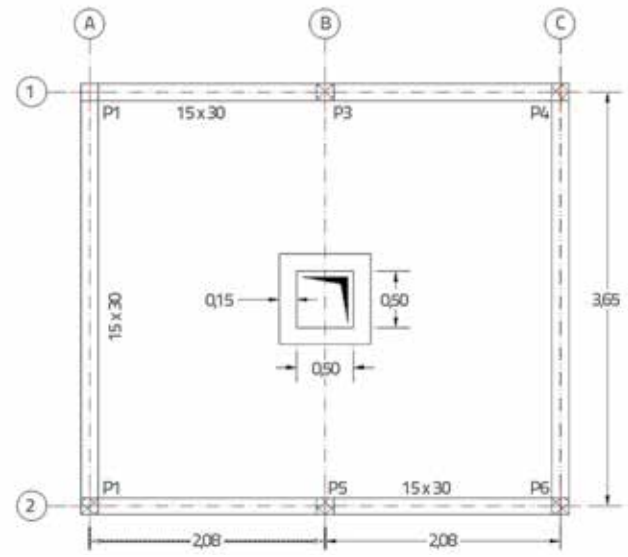

Figure 2. Plan view of tested structural model

After construction of the structure, accelerometers were placed on the structure to carry out the dynamic identification test by means of PCB Piezoelectric accelerometers. The accelerometers were located in opposite corners of the reinforced concrete frame so as to identify torsional mode and to capture longitudinal and transverse modes correctly. Two accelerometers were located on the first storey, and two accelerometers were located on the second storey. Accelerometer positions can be seen in Figure 3. Figure 3 shows position of accelerometers on the first storey. Two accelerometers were used in the north-eastern corner of the structure, and two accelerometers were used in the south-western corner of the structure. The same instrumentation technique was used for the second storey. Eight accelerometers in total were used for dynamic identification of this model on reinforced concrete frame. E_{inf}, υ_{inf}, ρ_{conc}, ρ_{infill} and f_{cm} values were obtained by experimental study [15]. These parameters are presented in Table 1. Initially, ρ_{conc} was defined by experiment, and subsequently the value E_{conc} was calculated according to Eurocode 2 [16].

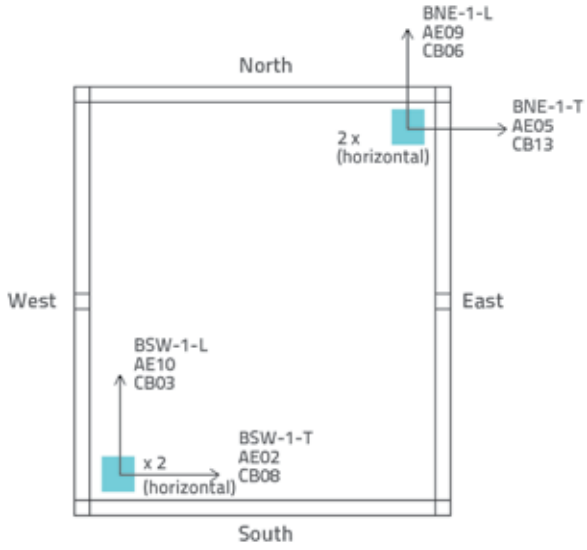

Figure 3. Instrumentation of accelerometers for first floor

3.2. Dynamic identification

According to experimental results, the first mode was identified in the following sequence; transverse, longitudinal, and rotational, while the fourth and fifth modes were mixed. Experimental modes and mode frequencies are shown in Figure 4 [14].

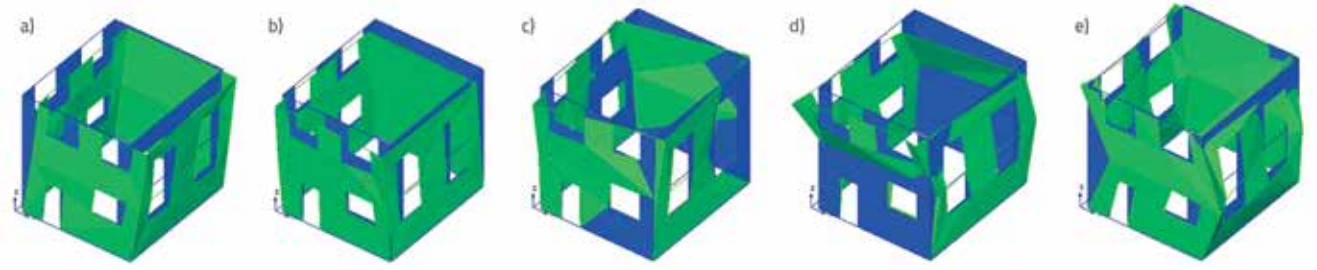

Figure 4. Experimental 5-mode shapes and frequencies a) 1st mode (f_1=7,71 Hz); b) 2nd mode (f_2=9,61 Hz); c) 3rd mode (f_3=26,9 Hz); d) 4th mode (f_4=32,8 Hz); e) 5th mode (f_4=39,4 Hz) [14]

3.3. Development of finite elements

The numeric model of Two Leaf Cavity Wall Reinforced Concrete Structure is constructed to check correctness of engineering parameters for the start of structural analysis. During the modelling of FE simulation of this structure, the columns, beams and foundation were modelled with the class-III beam elements that are defined in software as CL18B.This beam element is composed of three nodes. CL18B beam element is presented in Figure 5. The slab of the structure was modelled with the eight-node quadrilateral curved shell element defined as CQ40S in the software, as shown in Figure 6. All walls of the structure were modelled with the eight-node quadrilateral layered curved shell element defined as CQ40L in the software. This element can be seen in Figure 7. Interface elements were modelled around the infill. A three-node line to surface interface element was used. The name of this element, shown in Figure 8, is CL24I.

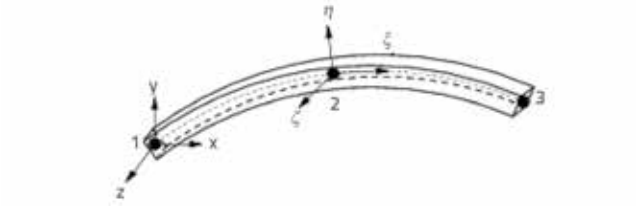

Figure 5. CL18B three-node curved beam element

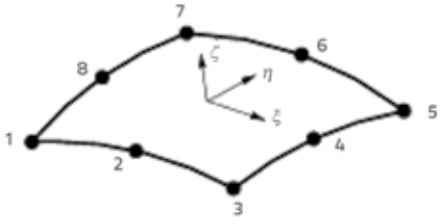

Figure 6. CQ40S eight-node curved shell element

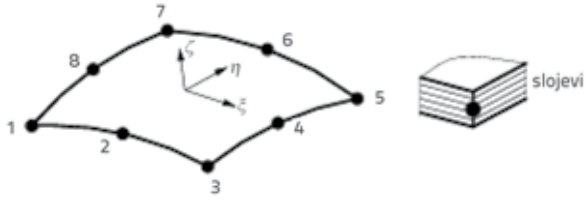

Figure 7. CQ40L eight-node layered curved shell element

Different modelling approaches are shown in Figure 9 [17]. A macro model was used when modelling strategies of the interface element. The basic assumption of the macro model is presented in Figure 9(d). The purpose of using the macro model is to simulate general behaviour of the infill wall. Thus, an interface element was used between the reinforced concrete frame and infill walls.

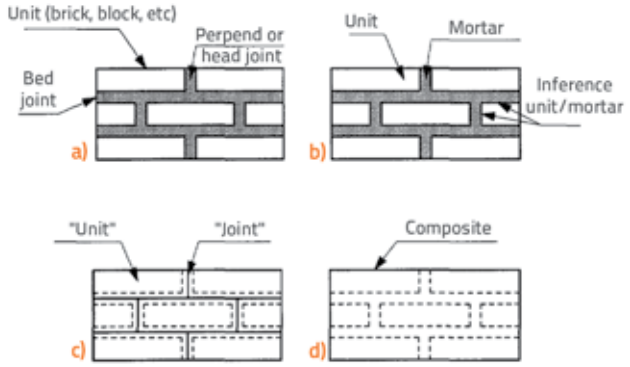

Figure 9. a) ordinary masonry sample, b) micro model with detailed approach, c) micro-model with simplified approach d) macro modelling of masonry [17]

The computation of interface stiffness at the contact between the reinforced concrete and infill wall is quite complicated. During the calculation, it is necessary to take into account the elastic modulus of brick unit, elastic modulus of mortar, and thickness of mortar. K_N and K_S of the interface element are calculated as shown below [17]. From this equation, K_N value is computed according to eq. (14):

$$K_N = \frac{E_u E_m}{t_m(E_u - E_m)} \tag{14}$$

The value E_u amounts to 30444 N/mm² for brick wall and 3135 N/mm² for mortar. The thickness of the joint is 20 mm. 175 N/mm was calculated for K_S. Then the value is calculated according to eq. (15) below:

$$K_S = \frac{K_N}{2x(1+\upsilon)} \tag{15}$$

In this equation, the value of 0.15 was adopted for υ. Thus, the value amounts to 75.25 N/mm. K_N (normal traction) was used for vertical direction of infill wall behaviour and K_S (shear traction) was used for horizontal direction of infill wall behaviour due to orthotropic type of infill wall material.

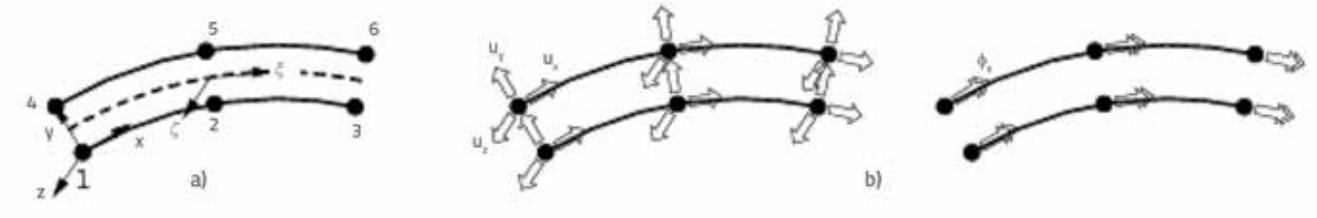

Figure 8. CL24I three-node line to shell interface element a) topology, b) displacement

4. Case study of two-leaf cavity brick infill wall

In this case study, the calibration was conducted using MATLAB with the least square algorithm minimization of objective function. To obtain the best match 10^{-6} is determined as the tolerance between the n^{th} and $(n-1)^{th}$ iteration numbers. When this tolerance is reached, the updating process stops automatically. The calibration process is conducted jointly by MATLAB [18] and DIANA 9.4.4 [19]. The flowchart of this calibration is shown in Figure 10.

The rigid foundation was used the first during the modal updating process. After calculating eigenvalues, it was realized that the first three modes were unfortunately oriented in the wrong direction. The elastic foundation was used to justify the mode shapes. This situation emerged because of the incomplete boundary condition. This problem is caused by connection between the foundation and the shake table. Vertical loads could not be fully supported, as shown in Figure 11. This problem was eliminated by using elastic foundation.

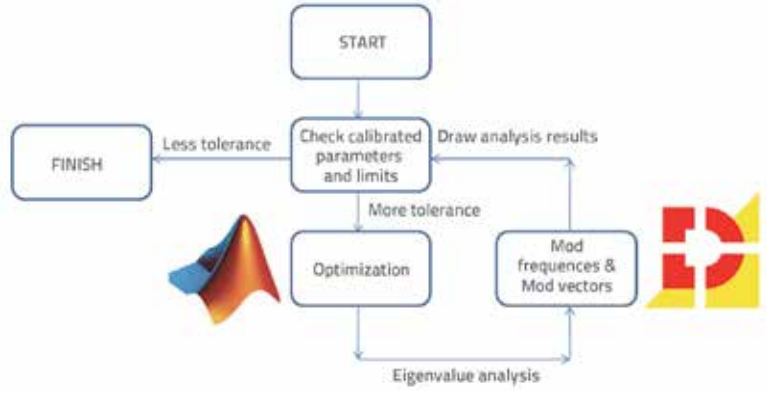

Figure 10. Flowchart of modal calibration

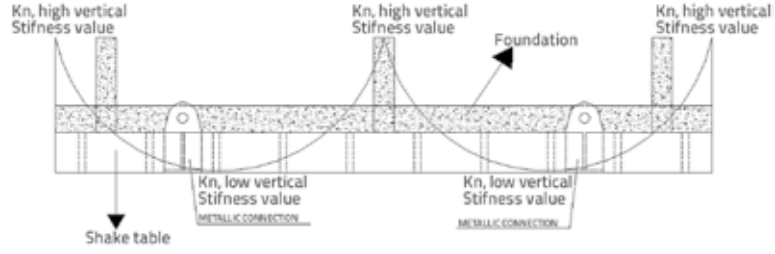

Figure 11. Stiffness variations along longitudinal axis of model

Two different elastic foundation properties were used under the foundations to simulate a shake table. One of the properties was used for the north and south direction, while the other one was used for west and east direction. However, this elastic foundation was used only to overcome the boundary condition problem, and not to simulate a shake table. Consequently, no engineering properties were available with regard to vertical stiffness of the shake table. These engineering properties were selected randomly. Correct mode shapes and mode frequencies after using elastic foundation before modal updating are shown in Figure 12.

Unfortunately, after the shake table experiment, as shown in Figure 12.c, the 3rd mode could not be justified even with the use of elastic foundation. However, during modal updating, it was focused on four modes. First transversal, first longitudinal and fourth, fifth mixed modes. Two different modal calibrations were conducted to obtain experimental frequencies. Mode shapes were greatly affected by the parameters, particularly stiffness of elastic foundation. For this reason, the first modal calibration was focused on elastic foundation. But movement capability was restricted due to distinct number of $K_{N(W-E)}$, $K_{N(N-S)}$ and $K_{S(ALL)}$. For this reason, the modal updating process was enlarged from the 1st order important parameters to the 2nd order important parameters.

4.1. Calibration number 1

Only normal stiffness of the north and south faces of the elastic foundation were calibrated in the calibration No. 1. The calibration process was stopped automatically at the seventh step. Calibration results are presented in Table 3.

As can be seen in Table 3, there were no considerable differences between frequencies of the fourth and fifth modes. The updating process was completed successfully but, unfortunately, calibration decreased the error from 5.135 % to 2.83 %. Related graphs and captured images can be seen in Figure 10 a, b, c, and d. As can be seen, there is a slight change at the second and fourth modes. For this reason, other calibration processes focused on these modes with different parameters.

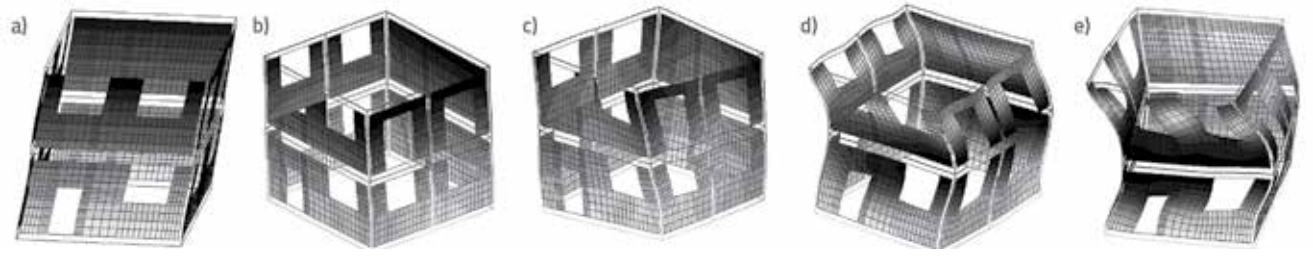

Figure 12. FEM modes and mode shapes: a) 1st mode FEM (f_1=8,14 Hz); b) 2nd mode FEM (f_2=9,87 Hz); c) 3rd mode FEM (f_3=23,89 Hz); d) 4th mode FEM (f_4=35,79 Hz); e) 5th mode FEM (f_5=40,8 Hz)

Table 3. Updating summary for calibration 1

Variables	Initial values [N/mm]	Updated values [N/mm]	Experimental frequencies (1)	Initial frequencies (2)	Error between (1) and (2) [%]	Updated frequencies (3)	Error between (1) and (3) [%]
$K_{N(W-E)}$	$1 \cdot 10^4$	$0.43 \cdot 10^4$	7.71	8.14	5.54	7.52	2.49
$K_{N(N-S)}$	$1 \cdot 10^5$	$0.9 \cdot 10^5$	9.61	9.87	2.6	9.66	0.43
			32.8	35.79	8.9	35.77	8.9
			39.4	40.8	3.5	40.79	3.5
				Average	5.135	Average	2.83

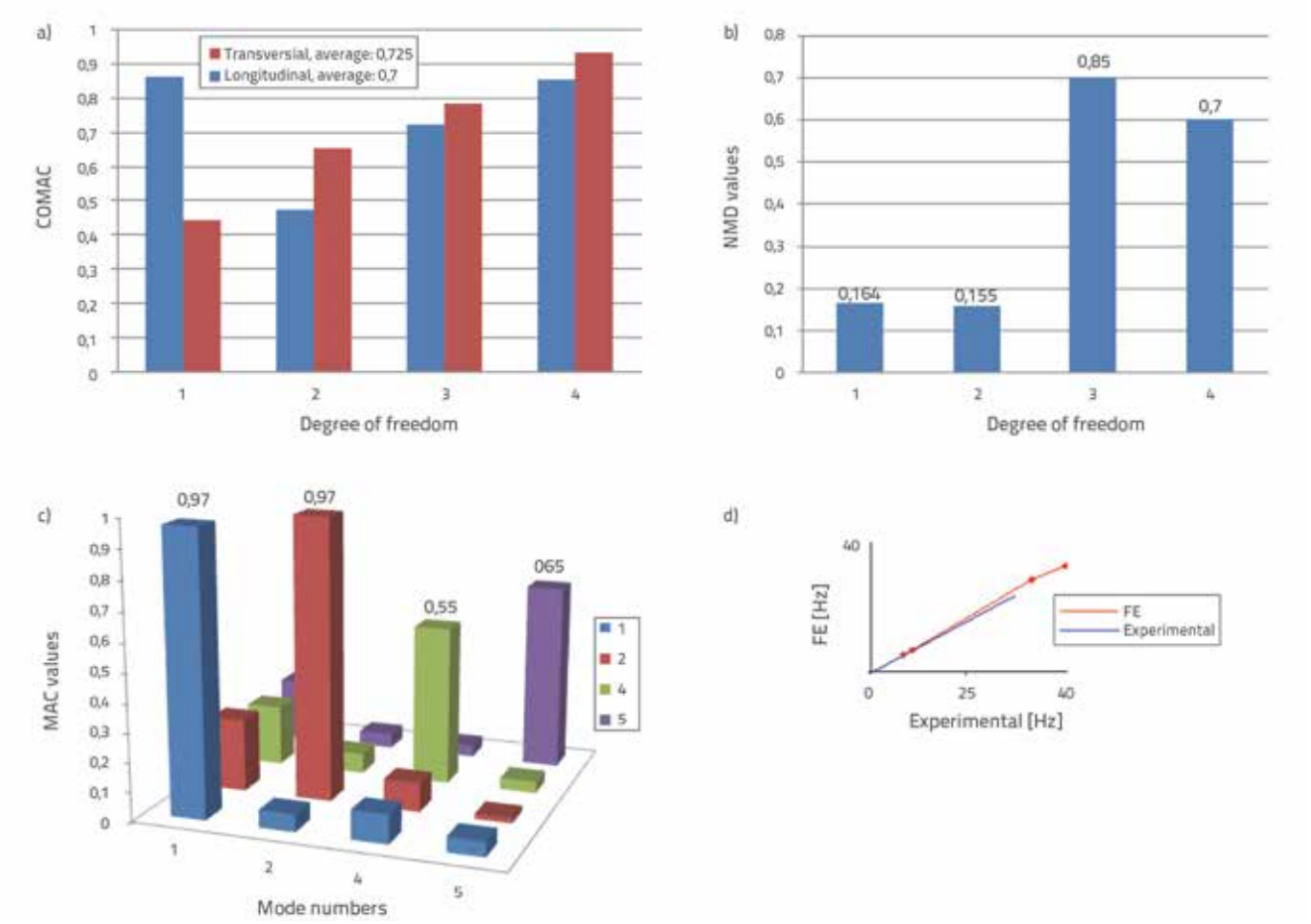

Figure 13. a) COMAC values, b) NMD values, c) MAC values, d) frequency comparison

Table 4. Updating summary for calibration 2

Variables	Initial values [N/mm]	Updated values [N/mm]	Experimental frequencies (1)	Initial frequencies (2)	Error between (1) and (2) [%]	Updated frequencies (3)	Error between (1) and (3) [%]
$K_{N(W-E)}$	$1 \cdot 10^4$	$7.6 \cdot 10^3$	7.7123	8.14	5.54	7.64	0.9
$K_{N(N-S)}$	$1 \cdot 10^5$	$8.52 \cdot 10^5$	9.6187	9.87	2.6	9.55	0.7
$K_{S(ALL)}$	$1 \cdot 10^8$	$9.75 \cdot 10^6$	32.842	35.79	8.9	35.74	8.8
			39.428	40.8	3.5	40.75	3.35
				Average	5.135	Average	3.44

4.2. Calibration number 2

In this calibration, in addition to $K_{N(W-E)}$ and $K_{N(N-S)}$, the shear stiffness of elastic foundation was also considered during the updating process. The calibration process was stopped at the seventh step. Results are given in Table 4.

4.3. Calibration number 3

Calibration parameters were increased in this calibration so as to obtain a better correlation. $K_{N(W-E)}$, $K_{N(N-S)}$, $K_{S(ALL)}$, $K_{N(interface)}$ and $K_{S(interface)}$, were considered. Calibration was stopped automatically at the tenth step. Results are presented in Table 5.
As can be seen in calibration Table 5, the correlation is better because of five parameters. An increase in the number of parameters also increases reliability of the updating process. In this calibration, a special emphasis was placed on the first two modes. Convergences of the first two modes amount to less than 1 %. However, the last two modes are slightly less favourable due to restricted moving capacity of elastic foundation.

4.4. Calibration number 4

K_{inf}, $K_{N(interface)}$ and $K_{S(interface)}$ were considered in this calibration so as to analyse the convergence of calibration. Mode shapes and mode frequencies were extremely influenced by experimental value of the modulus of elasticity and by calculated parameters of normal and shear traction. That is why these parameters were calibrated to obtain convergence. This calibration was stopped automatically at the tenth step. The corresponding results are given in Table 6.
Table 6 shows that the calibration of E_{inf} and stiffness values of the interface element does not bring a better correlation after the updating process, compared to other calibrations. Because E_{inf} is an experimental value, the shear and normal traction of the interface element is calculated by the formula proposed by Lourenço [10]. This calibration shows that these values have to be fixed.

Table 5. Updating summary for calibration 3

Variables	Initial values [N/mm]	Updated values [N/mm]	Experimental frequencies (1)	Initial frequencies (2)	Error between (1) and (2) [%]	Updated frequencies (3)	Error between (1) and (3) [%]
$K_{N(W-E)}$	$1 \cdot 10^4$	$0.05 \cdot 10^4$	7.7	8.1	5.5	7.4	3.8
$K_{N(N-S)}$	$1 \cdot 10^5$	$1.1 \cdot 10^5$	9.6	9.8	2.6	9.6	0.3
$K_{S(ALL)}$	$1 \cdot 10^5$	$5 \cdot 10^5$	32.8	35.8	8.9	34.2	4.0
$K_{N(interface)}$	$1.75 \cdot 10^8$	$10.5 \cdot 10^8$	39.4	40.8	3.5	39.5	0.1
$K_{S(interface)}$	$75.52 \cdot 10^7$	$10.1 \cdot 10^7$					
				Average	5.1	Average	2.0

Table 6. Updating Summary for Calibration 4

Variables	Initial values [N/mm]	Updated values [[N/mm]	Experimental frequencies (1)	Initial frequencies (2)	Error between (1) and (2) [%]	Updated frequencies (3)	Error between (1) i and (3) [%]
E_{inf} [N/mm^2]	$3.6 \cdot 10^6$	$3.1 \cdot 10^6$	7.7	8.1	5.5	8.1	5.1
$K_{N(interface)}$ [N/mm]	$1.7 \cdot 10^8$	$10.5 \cdot 10^8$	9.6	9.9	2.6	9.7	0.6
$K_{S(interface)}$ [N/mm]	$75.2 \cdot 10^7$	$231.8 \cdot 10^7$	32.8	35.8	8.9	34.4	4.6
			39.4	40.8	3.5	39.0	0.98
				Average	5.135	Average	2.83

Table 7. Updating summary for calibration 5

Variables	Initial values [kN/mm^2]	Updated values [kN/mm^2]	Experimental frequencies (1)	Initial frequencies (2)	Error between (1) and (2) [%]	Updated frequencies (3)	Error between (1) and (3) [%]
E_{inf}	$3.6 \cdot 10^6$	$3.3 \cdot 10^6$	7.7	8.1	5.5 %	8.0	3.7
E_{conc}	$3.04 \cdot 10^7$	$2.35 \cdot 10^7$	9.6	9.8	2.6 %	9.5	0.7
			32.8	35.7	8.9 %	33.9	3.2
			39.4	40.8	3.5 %	38.5	2.3
				Average	5.1 %	Average	2.4

Table 8. Comparison of this study with references

Item \ References	Ramos et al. (2010)	Li et al. (2011)	Sevim et al. (2011)	Atamtürktür (2009)	This study
Purpose of modal calibration	Model structure error	Incomplete modal data	Model parameter error	Model structure error	Model structure error
Problem at FE model	Huge differences at mode frequencies between FE and experiment	Unable to obtain accurate dynamic model	Unable to obtain correct FE model according to in-situ Measurement	Unable to measure reliability of simplified geometry & Unable to obtain reliable model due to mesh number	Unable to obtain correct mode shape & to verify tested material data
Solution	Using interface stiffness under foundation	calibration of stiffness matrix	Calibration of estimated parameters to obtain experimental frequencies	Tried to obtain equal area and moment of inertia for simplification & multiple analysis with different mesh numbers	Using flexible boundary under foundation and calibration of experimental parameters
Average match before & after calibration between mode frequencies	Before = 0.60 After = 0.97	Before = 0.93 After = 0.99	Before = 0.9 After = 0.95(for Osmanlı Bridge) Before = 0.85 After = 0.99 (for Şenyuva Bridge)	Displacement based final convergence = 0.98 Match between coarse&fine mesh = 0.88	Before = 0.94 After = 0.98 Moreover correct mode shape

4.5. Calibration number 5

This calibration process is implemented by E_{inf} and E_{conc} parameters. These two experimental parameters were obtained by Pereira [15]. The purpose of this calibration 5 is to evaluate calibration results of the elastic modulus of infill and concrete. Tabulated results show that these parameters do not exert a great influence on calibration because error could be decreased by approximately 2.5 % only. This calibration process was completed automatically at the seventh step. The final calibration can be seen in Table 7.

After model calibration, it is important to compare the results with references. This comparison is presented in Table 8.

5. Conclusion

This paper presents an adaptive solution for updating structural model of a RC structure with the two-leaf cavity brick infill wall under a flexible boundary problem. The flexible boundary problem occurred due to degradation of local stiffness at the position where structural foundation was fixed to the shake table. To eliminate this problem, the elastic foundation was modelled under structural foundation as an interface element. Then, the modal updating process was performed on the "Two Leaf Cavity Wall Reinforced Concrete Structure" by deterministic approach. The forced vibration test was performed on the structure before the shake table test, in order to identify the mode frequencies and mode shapes. After modelling this structure with the finite element software DIANA 9.4.4 (2012), the eigenvalue analysis was performed on the model. After the eigenvalue analysis, the mode shapes of the first three finite-element modes were completely different from the experimental mode shapes. This difference was the evidence of a boundary condition problem. Similar structural problems were reported by Ramos et al. (2010) [7] and Atamtürktür (2009) [9]. The main objective of this paper is to find the reason of this inappropriate condition and to eliminate it. The reason behind this problem was investigated and it was established that this is a flexible boundary condition problem due to degradation of stiffness at foundation level. This degradation of stiffness occurred at the position where the structure is connected to the shake table. The novelty of this study lies in bypassing this local stiffness degradation of foundation by means of an elastic foundation. This was done because it was observed after eigenvalue analysis that the first three modes were incorrect with rigid foundation, even if experimental material properties were used. This huge specimen was cast outside of the shake table and was then moved to the shake table to expose it to earthquake load. After that, the specimen was connected to shake table with metallic supports as shown in Figure 8. These connection points decreased vertical stiffness of the structure. Finally, the modal updating was started. Modal calibration is the second objective of this paper. This calibration process was divided into five steps. At the end of the five-step calibration process, it can easily be seen from the summary table of each calibration that the difference between individual calibration stages is not significant. These five calibrations showed that experimental material properties such as E_{inf} and E_{conc}, and the calculated shear and normal traction of interface values, based on proposed formula, are reliable. After this calibration, it can be concluded that an average error before updating was 5,1 % and, after updating, the frequency error decreased to 2,83 %, 3,44 %,

2,0 %, 2,83 % and 2,4 %, respectively. High correlation between the experimental and numeric values was achieved by calibration 3 due to the smallest average error of 2 % as obtained at the end of the calibration. The reason behind the smallest average error at calibration 3 lies *inter alia* in the use of five parameters during calibration 3. All these five parameters were calculated, i.e. they were not obtained experimentally. The finite element model of the structure was adapted to the best experimental modal position by calibrating five calculated stiffness values at calibration 3. However, the third experimental mode shape of the structure could not be obtained by the finite element model because the movement capability of the structure was restricted by stiffness properties of elastic foundation aimed at eliminating an inappropriate condition. This inappropriate or ill condition prevented the structure from simulating the third mode. First two modes of the structure were adjusted but, unfortunately, it was impossible to correct the third mode. Due to elastic foundation, the NMD value as a modal updating match indicator is somewhat high when compared to literature results. These undesired high values were registered for the fourth and fifth modes only. Finally, this study has proven that the model structure error can also occur during the ex-situ test performed in laboratory, i.e. not only in-situ test performed in the field, like in the study contributed by Ramos et al. (2010). The deterministic modal updating process is needed to overcome this type of structural problem and to prepare a reliable model with reliable material properties before starting any type of structural analysis.

REFERENCES

[1] Atamtürktür, S., Laman, J.A.: Finite element model correlation and calibration of historic masonry monuments: review. *The Structural Design of Tall And Special Buildings*, 21 (2010), pp. 96-113, https://doi.org/10.1002/tal.577

[2] Sevim, B., Bayraktar, A., Altunışık, A.C., Atamtürktür, S., Birinci, F.: Finite element model calibration effects on the earthquake response of masonry arch bridges, *Finite Element in Analysis and Design*, 47 (2011), pp. 621-634, https://doi.org/10.1016/j.finel.2010.12.011

[3] Cunha, A., Caetano, E.: Experimental Modal Analysis Of Civil Engineering Structures, *Journal of Sound and Vibration*, pp. 12-20, June, 2006.

[4] Mottershead, J.E., Friswell, M.I.: Modal Updating In Structural Dynamics: A Survey, *Journal of Sound and Vibration*, pp. 347-375, 1993, https://doi.org/10.1006/jsvi.1993.1340

[5] Friswell, M.I., Mottershead, J.E., Ahmadian, H.: Finite-Element Model Updating Using Experimental Test Data: Parametrization And Regularization, *The Royal Society*, pp. 169-186, 2001.

[6] Khodaparast, H.H., Mottershad, J.E., Friswell, M.I.: Perturbation Methods for The Estimation of Parameter Variability in Stochastic Model Updating, *Mechanical Systems and Signal Processing*, 22 (2008), pp. 1751–1773, https://doi.org/10.1016/j.ymssp.2008.03.001

[7] Ramos, L.F., Alaboz, M., Aguilar, R.: Dynamic Identification and Monitoring of St. Torcato Church, *Advanced Material Research,* 133-134 (2010), pp. 275-280, https://doi.org/10.4028/www.scientific.net/AMR.133-134.275

[8] Li, H.J., Wang, J.R., Hu, S.L.J.: Modal Updating Based on Incomplete Modal Data, *Sci China Tech Sci*, 54 (2011), pp. 1737-1747, https://doi.org/10.1007/s11431-011-4415-z

[9] Atamtürktür, S.: Verification And Validation Under Uncertainty Applied To Finite Element Models Of Historic Masonry Monuments, *Proceedings of the IMAC-XXVII*, Orlando, Florida USA, 2009

[10] Wang, W., Mottershead, J. E., Mares, C.: Mode-shape Recognition and Finite Element Model Updating Using the Zernike Moment Descriptor, *Mechanical System and Signal Processing,* 23 (2009), pp. 2088-2112, https://doi.org/10.1016/j.ymssp.2009.03.015

[11] Allemang, J.R.: The Modal Assurance Criterion – Twenty Years Of Use And Abuse, *Sound and Vibration*, pp. 14-21, 2003.

[12] Ramos, L.F.: Damage Identification On Masonry Structures Based on Vibration Signatures, *PhD Thesis*, Guimaraés, Universidade do Minho, 2007.

[13] Douglas, B., Reid, W.: Dynamic Tests And System Identification of Bridges, *Journal of the Structural Division*, 108 (1982) 10, pp. 2295-2312.

[14] Leite, J.K.: Seismic Behaviour of Infill Walls: Design And Testing, *PhD Thesis*, Universidade of Minho, Guimaraés, Portugal, 2014.

[15] Pereira, M.F.P.: Avaliação Do Desempenho Das Envolventes Dos Edifícios Face À Acção Dos Sismos, *PhD Thesis*, Universidade do Minho, Guimaraés, Portugal, 2013.

[16] Eurocode 2: Design of Concrete Structures - Part 1-1: General Rules and Rules for Buildings, EN 1992-1-1, December 2004.

[17] Lourenço, P.B.: Computational Strategies for Masonry Structures, *PhD Thesis*, Delft, Netherland, 1996.

[18] MATLAB, MATLAB: The Language of Technical Computing, The MathWorks, Release 7.2, USA, 2006.

[19] TNO, DIsplacement method ANAlyser, *User's Manual, Release 9.4.4*, Netherlands, 2012.